JACS JOURNAL OF THE AMERICAN CHEMICAL SOCIETY

Article

Cite This: J. Am. Chem. Soc. 2018, 140, 16855−16864

pubs.acs.org/JACS

Unlocking a Diazirine Long-Lived Nuclear Singlet State via Photochemistry: NMR Detection and Lifetime of an Unstabilized Diazo-Compound

Barbara Procacci,[†] Soumya S. Roy,[†] Philip Norcott,[†] Norman Turner,[‡] and Simon B. Duckett*[,†]

[†]Centre for Hyperpolarisation in Magnetic Resonance, Department of Chemistry, York Science Park, University of York, York YO10 5NY, United Kingdom

[‡]Accelerator Research Group, University of Huddersfield, Queensgate, Huddersfield HD1 3DH, United Kingdom

Supporting Information

ABSTRACT: Diazirines are important for photoaffinity labeling, and their photoisomerization is relatively well-known. This work shows how hyperpolarized NMR spectroscopy can be used to characterize an unstable diazo-compound formed via photoisomerization of a $^{15}N_2$-labeled silyl-ether-substituted diazirine. This diazirine is prepared in a nuclear spin singlet state via catalytic transfer of spin order from *para*-hydrogen. The active hyperpolarization catalyst is characterized to provide insight into the mechanism. The photochemical isomerization of the diazirine into the diazo-analogue allows the NMR invisible nuclear singlet state of the parent compound to be probed. The identity of the diazo-species is confirmed by trapping with *N*-phenyl maleimide via a cycloaddition reaction to afford bicyclic pyrazolines that also show singlet state character. The presence of singlet states in the diazirine and the diazo-compound is validated by comparison of experimental nutation behavior with theoretical simulation. The magnetic state lifetime of the diazo-compound is determined as 12 ± 1 s in CD_3OD solution at room temperature, whereas its chemical lifetime is measured as 100 ± 5 s by related hyperpolarized NMR studies. Indirect evidence for the generation of the photoproduct *para*-N_2 is presented.

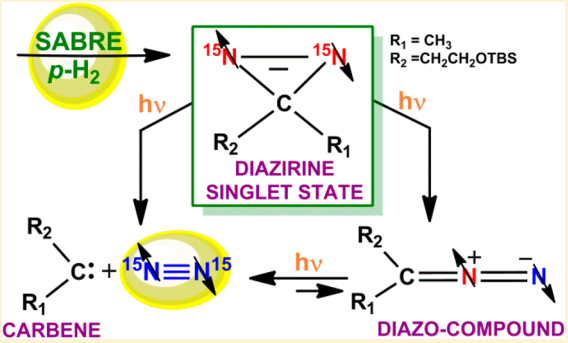

INTRODUCTION

Diazirines exhibit significant photochemistry,[1−3] and their photoisomerized diazo-products are versatile tools employed in chemical synthesis[4] and chemical biology.[5−7] In fact, their complex reactivity has interested the physical chemistry community for many years, with the importance of these compounds having increased due to their proven capabilities as good photoaffinity probes and molecular tags.[8−14] Recently, the successful hyperpolarization of $^{15}N_2$-diazirines via the SABRE-SHEATH (Signal Amplification By Reversible Exchange in Shield Enables Transfer to Heteronuclei) hyperpolarization technique has dramatically widened their relevance as it established that their ^{15}N NMR signals can be enhanced to the point where they should be observable by in vitro or in vivo magnetic resonance imaging (MRI).[15,16] In this Article, we exploit SABRE to prepare the diazirine in selected nuclear spin orientation and identify a diazirine complex as the active catalyst. We then use photoisomerization to produce the diazo-product, which is now available to NMR detection. We characterize this unstable intermediate and probe its kinetic evolution by NMR spectroscopy. Furthermore, we trap it by a 1,3 dipolar cycloaddition reaction, with singlet state retention, to provide further reaction rationalization. We finally discuss how this photochemical pathway can lead to the generation of *para*-N_2.

The two main photochemical pathways of diazirines that have been experimentally established by matrix photochemistry[17−19] and laser flash photolysis[20,21] (351 nm) correspond to the generation of a carbene with concomitant N_2 extrusion (Scheme 1a), and photoisomerization to a linear diazo-isomer[22] (Scheme 1b). The resulting diazo-species have

Scheme 1. Main Photochemical Pathways of Diazirines and Diazo-Compounds

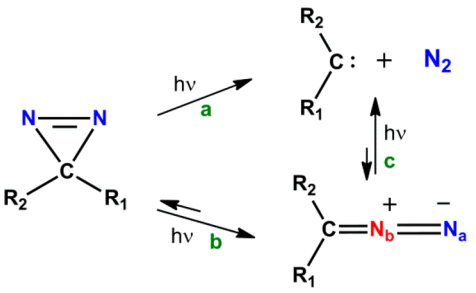

Received: October 10, 2018
Published: November 8, 2018

DOI: 10.1021/jacs.8b10923
J. Am. Chem. Soc. 2018, 140, 16855−16864

been observed to decompose into a carbene and N_2 gas as a result of secondary photolysis (Scheme 1c). Experimental studies of matrix photochemistry and theoretical calculations convincingly demonstrated that the formation of the diazo-isomer can take place through recombination of the carbene and N_2.[17] However, this photoprocess is again wavelength dependent with shorter or longer wavelengths favoring isomerization or N_2 ejection depending on the reaction conditions or diazirine substitution pattern.[23] While parent alkyldiazirines are stable compounds in solution, their diazo-analogues are very labile species, and as a consequence their trapping is often difficult, requiring the use of special methods.[1]

Diazirines are a special class of cyclic-azo compounds in which the electrons in the HOMO are located on the N atoms to just ~55% with the remainder being delocalized within the molecule.[24,25] Thus, diazirines are poor coordinating ligands, and very few of their metal complexes have been reported. For instance, the diazirine complex $[(NH_3)_5Ru(N_2C_6H_{10})]^{2+}$ was prepared by reacting $[(NH_3)_5Ru(H_2O)]^{2+}$ with a stoichiometric amount of 3,3-pentamethylenediazirine under argon; coordination via a single nitrogen was established by X-ray crystallography, but no spectroscopic characterization in solution was achieved as rapid oxidation took place to yield the dinitrogen-Ru analogue and cyclohexanone.[26] Non-acarbonyldiiron $Fe_2(CO)_9$ was also reported to react with 3,3-dimethyldiazirine in tetrahydrofuran to afford a relatively unstable complex in which two $Fe(CO)_4$ groups were each σ-bound to a nitrogen atom of the diazirine (Scheme 2a). This

Scheme 2. Reported Dimethyldiazirine Coordination Modes Illustrated for Two Iron Centers[a]

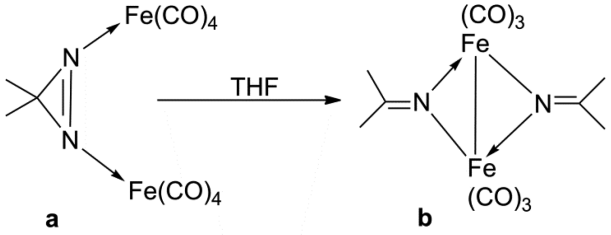

[a]THF plays a role in the solution-based decomposition to (b), which forms a structure with two dimethylketiminato groups.[27]

complex was found to decompose slowly in solution affording complexes of the type shown in Scheme 2b where two molecules of diazirine have reacted with the loss of N_2 and then coordinated to the Fe center.[27] Cu(110) and Pd(110) surfaces have been employed to study the dissociative adsorption of diazirines at 124 K, and, while selective NN bond scission took place at Cu, both NN and CN bond scission were observed for Pd.[28,29] In fact, most of the reactions between diazirines and a metal complex seem to afford a metal-carbene species via diazirine decomposition to the reactive carbene and N_2.[30−33]

SABRE is a non hydrogenative PHIP (Para Hydrogen Induced Polarization) technique that builds on the earlier work of Bowers, Weitekamp, Eisenberg, and Bargon.[34,35] It relies on the reversible binding to a suitable metal complex of both *para*-hydrogen (p-H_2) and, in this case, a diazirine, to mediate hyperpolarization transfer into the free ligand.[36] The SABRE-SHEATH variation uses a lower-field condition to build up ^{15}N diazirine polarization efficiently. It has also been reported to create long-lasting signals that remain visible for 5.8 min after storage at 120 G in the case of 2-cyano-3-(d_3-methyl-$^{15}N_2$-diazirine)-propanoic acid with >10 000-fold signal enhancements. Furthermore, a long-lived nuclear singlet spin order was created between the pair of chemically inequivalent ^{15}N nuclei in this $^{15}N_2$-labeled diazirine whose lifetime was 23 min at 3 G. However, when the same experiment was repeated at a 10 000 G (1 T) storage field, the lifetime reduced drastically to 12 s.[15] Measurement of the hyperpolarized signal lifetimes of the diazirine as a function of substitution pattern gave useful insights into the magnetization transfer mechanism of SABRE-SHEATH, but the active SABRE species were not characterized experimentally, although possible products involving different coordination modes were proposed.[16] Recently, $^{15}N_4$-1,2,4,5-tetrazines were hyperpolarized via this approach and prepared in different spin orders. In addition, the bioorthogonal reaction of this species with cyclooctyne afforded hyperpolarized products. Indirect evidence for the generation of *para*-$^{15}N_2$ gas was also presented.[37]

RESULTS

SABRE-SHEATH Mechanism. This study employed the SABRE catalyst Ir(d_{22}-IMes)(COD)(Cl) **1** (where the IMes ligand is fully deuterated except for the pair of imidazolyl protons), and it involved examination of the silyl-ether-substituted diazirine **2** labeled with $^{15}N_2$ by ^1H NMR spectroscopy under SABRE and SABRE-SHEATH conditions (Scheme 3). To do this, solutions of **1** (5 mM) in the presence

Scheme 3. Structures of the Iridium Precatalyst 1 (Mesityl Groups Are Fully Deuterated) and the Silyl-Ether-Substituted Diazirine 2 Labeled with $^{15}N_2$

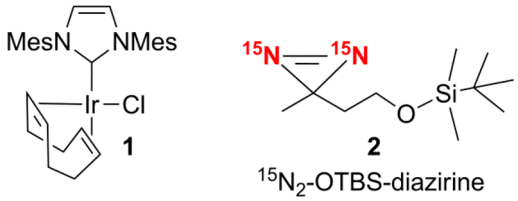

of excess pyridine-d_5 (200 mM) and excess **2** (150 mM) were utilized. Pyridine plays a role as a coligand in this process and is essential to the formation of the active SABRE catalyst. These CD_3OD (0.5 mL) solutions were activated via the addition of p-H_2 (4 bar) to the NMR tube prior to monitoring.

The SABRE-SHEATH process was then undertaken under conditions similar to those reported by Shen et al.[16] Briefly, the solution was either manually shaken or bubbled for 20 s inside a μ-metal shield (at ~0.5 μT measured by a milliGauss meter). These experimental conditions allowed hyperpolarization to be transferred from p-H_2 to the ^{15}N nuclei of **2** through SABRE (δ 465, Figure 1a,b). In addition to ^{15}N sensitization, hyperpolarization is also transferred to the proton resonances of the CH_3 and CH_2 alkyl groups that are adjacent to the ^{15}N center of **2** (Figure 1c). As these ^1H resonances fail to show hyperpolarization when the sample is shaken outside the μ-metal shield, we conclude that this effect results from relayed transfer via the iridium hydrides formed by oxidative addition of p-H_2 to the Ir precatalyst and the two ^{15}N centers (see the Supporting Information). A peak for bound diazirine in the SABRE transfer catalyst is observed at δ 299 in the $^{15}N\{^1H\}$

DOI: 10.1021/jacs.8b10923
J. Am. Chem. Soc. 2018, 140, 16855−16864

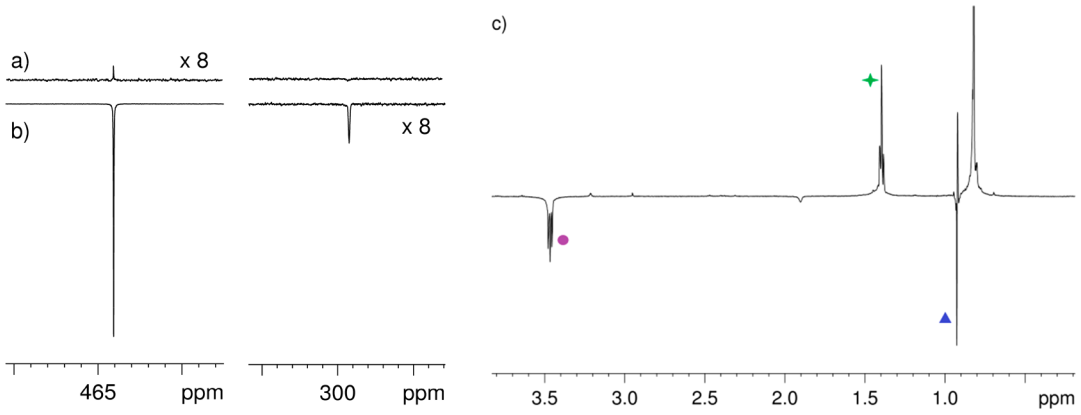

Figure 1. Left: $^{15}N\{^{1}H\}$ NMR spectra from a reaction mixture of **1**, **2**, and pyr-d_5 under p-H_2 atmosphere in CD_3OD. (a) Thermal reference NMR spectrum acquired with 1 scan and magnified (×8). (b) Corresponding hyperpolarized spectrum acquired identically after the sample was shaken with p-H_2 inside a μ-metal shield. (c) Corresponding single scan ^{1}H hyperpolarized NMR spectrum; the CH_3 (blue ▲) and CH_2 protons (purple ● and green star) of diazirine **2** receive hyperpolarization via transfer from ^{15}N after the sample is shaken in a μ-metal shield.

spectrum (Figure 1b), and the following measurements secured its identity.

Inspection of the hydride region of the ^{1}H NMR spectra recorded in CD_3OD at 298 K under both SABRE and SABRE-SHEATH conditions (p-H_2 bubbled at 298 K) showed two broad peaks with chemical shifts indicating hydrides positioned *trans* to ^{15}N (Figure 2a). In addition, resonances for the known

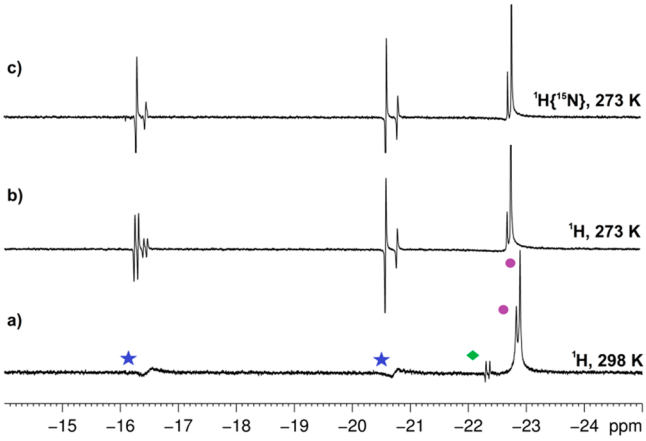

Figure 2. Hydride region of a series of ^{1}H NMR spectra of a reaction mixture of **1**, **2**, and pyr-d_5 in CD_3OD under ∼4 bar of p-H_2 pressure indicating the formation of **3** (blue ★). The purple ● correspond to $[Ir(H)_2(d_{22}\text{-IMes})(\text{pyr-}d_5)_3]Cl$ and its H/D analogue. The product indicated by the green ◆ is unidentified, and it is not detected at low temperature: (a) ^{1}H NMR spectrum at 298 K; (b) ^{1}H NMR spectrum at 273 K; and (c) $^{1}H\{^{15}N\}$ NMR spectrum at 273 K.

$[Ir(H)_2(d_{22}\text{-IMes})(d_5\text{-pyr})_3]Cl$[38] are seen at δ −22.7 alongside a minor signal for its hydride-deuteride analogue at δ −22.6. The broad nature of the new resonances suggested dynamic behavior, and hence experiments were repeated with NMR detection at low temperature. These broad resonances sharpened at 273 K resolving into four signals arising from structurally similar species in a 4:1 ratio. Resonances for the major compound were observed at δ −20.5 (antiphase doublet of doublets, J_{HH} = 7.8 Hz, J_{NH} = 31.8 Hz) and δ −16.2 (antiphase doublet, J_{HH} = 7.8 Hz); the minor species displayed peaks at δ −20.7 (antiphase doublet of doublets, J_{HH} = 9.3 Hz, J_{NH} = 31.4 Hz) and δ −16.4 (antiphase doublet, J_{HH} = 9.3 Hz) (Figure 2b). The doublets of doublets simplified to an antiphase doublet retaining only J_{HH} coupling when ^{15}N decoupling was applied (Figure 2c). All of the resonances exhibited p-H_2-induced hyperpolarization. On the basis of these observations, we assigned these two compounds to two isomeric forms of the iridium dihydride complex **3** shown in Scheme 4.

The two isomers of **3** are the active catalysts for SABRE as they possess one hydride that lies *trans* to a pyridine (resonances at lower δ) and the other hydride that lies *trans* to a ^{15}N-labeled diazirine (resonances at higher δ that display ^{15}N splitting). This experimental evidence agrees with previously reported DFT (Density Functional Theory) calculations that indicate η^1 single-sided N-coordination.[15] The two isomers **3a** and **3b** arise from binding of the Ir-center to one of the ^{15}N centers of the diazirine, which renders them inequivalent. The two forms interconvert rapidly at room temperature such that broad hydride signals result (Scheme 4). The hopping of the Ir center from one ^{15}N to the other is slowed at 273 K to the point where these two species become well distinguished. The formation of **3**, and identical dynamic behavior, was observed when a similar reaction mixture was activated and analyzed on a larger scale via a flow reactor.[39,40] Species related to **3** are also observed when a diazirine was employed in which the OTBS group of **2** is replaced by a carboxylic acid moiety (see the Supporting Information). Complex **3** is, to the best of our knowledge, the first example of a diazirine metal complex that has been characterized in solution by NMR spectroscopy where coordination to iridium proceeds through a single nitrogen atom. A theoretical analysis of the structure and J-coupling network associated with **3** is provided in the Supporting Information; although the reported theory has been described before,[15] we include it to allow the reader to gain a better understanding of the experiments.

Photochemistry. A reaction mixture analogous to that described earlier was prepared and activated by bubbling p-H_2 through the solution in the mixing chamber for 10 min. The hyperpolarization transfer process was then performed in a μ-metal shield (SABRE-SHEATH). Under these conditions, large signal enhancements were observed for the ^{15}N response of **2** as already reported by Shen *et al.*[16] For comparison purposes, the signal-to-noise ratio (SNR) in the corresponding 128 scan thermal reference spectrum was measured to be ≃7,

DOI: 10.1021/jacs.8b10923
J. Am. Chem. Soc. 2018, 140, 16855−16864

Scheme 4. (Top) Differential Ligand Binding in 3 Leading to 3a and 3b, Which Rapidly Interconvert at Room Temperature; and (Bottom) Key NMR Spins System Parameters for 3

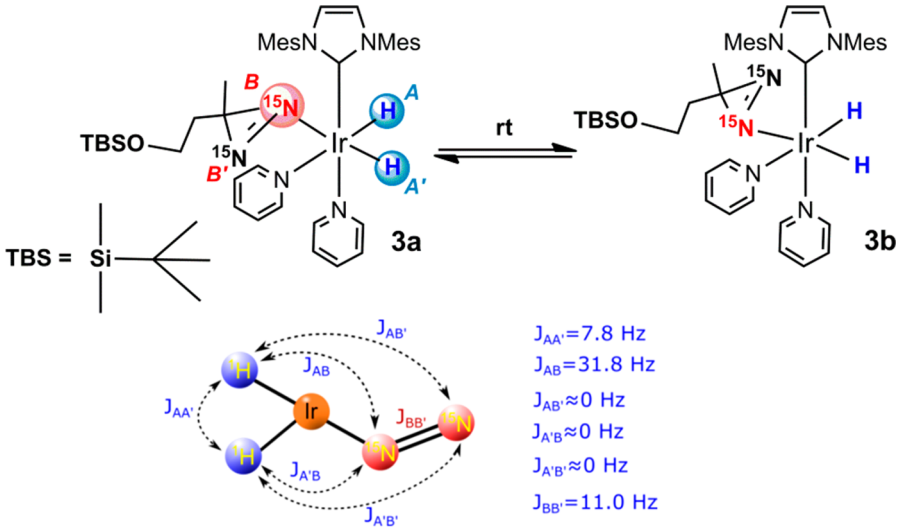

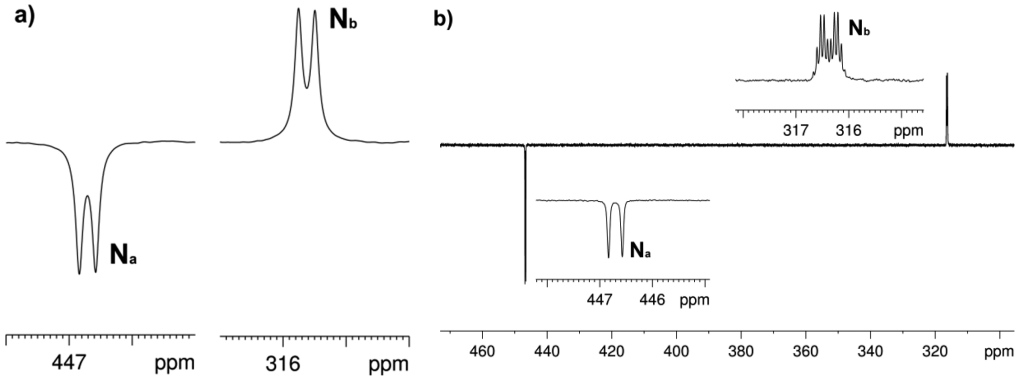

Figure 3. (a) $^{15}N\{^1H\}$ NMR spectrum of a CD_3OD hyperpolarized solution of **1**, **2**, and pyr-d_5 after 20 s broadband photolysis displaying resonances for **4**. (b) ^{15}N NMR spectrum of the same solution.

while it became ≃230 in the single scan hyperpolarized spectrum. Zeeman polarization associated with **2** is therefore measured via this process.

The hyperpolarization of the $^{15}N_2$-labeled-diazirine **2** will be the result of a mixture of direct polarization (SABRE-SHEATH) and singlet state transfer under ultralow magnetic field (mG). However, at relatively higher magnetic fields (1−1000 G), the formation of the singlet will be dominant with negligible contribution from direct magnetization.[15] Furthermore, the singlet form can have a remarkably long magnetic state lifetime due to its symmetric character as exemplified by p-H_2 whose reported lifetime is several months.[37,41] However, it must be noted that because pure singlet states are nonmagnetic, they cannot be detected directly by NMR until their symmetry is broken.

We achieve symmetry breakage by irradiating the sample in a quartz mixing chamber, which is at the Earth's magnetic field, with a broadband UV−vis lamp (either at λ > 290 nm or λ > 345 nm) for 20 s while p-H_2 is bubbled through it. After this time, photolysis is stopped, and the solution is transferred into the NMR spectrometer (transfer time ≃ 2 s). A new hyperpolarized compound is then detected with an excellent SNR (≃165, 1 scan) by $^{15}N\{^1H\}$ NMR spectroscopy. Furthermore, a control experiment performed without irradiation confirmed this species as a photoproduct of **2**. The new compound displayed two inequivalent nitrogen environments that are coupled to each other (δ 447 and δ 316, J_{NN} = 11 Hz) (Figure 3a). Interestingly, when the experiment was repeated without ^1H decoupling, the ^{15}N peak at lower δ appeared as a doublet of sextets (Figure 3b). This fine structure suggested that one of the two inequivalent nitrogen centers interacts with the five nearby proton environments of CH_2 and CH_3 groups via a J_{NH} coupling of 2.7 Hz. On the basis of these observations, we assign the new species to the predicted photoisomerization product alkyl diazo-**4** of Scheme 5 where the signal at δ 316 can be assigned as the one corresponding to the N in the position α to carbon (N_b,

Scheme 5. Structure of the Diazo-Compound 4 Formed by Photoisomerization of the ^{15}N Labeled Diazirine, 2

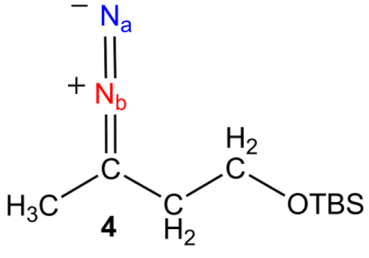

DOI: 10.1021/jacs.8b10923
J. Am. Chem. Soc. 2018, 140, 16855−16864

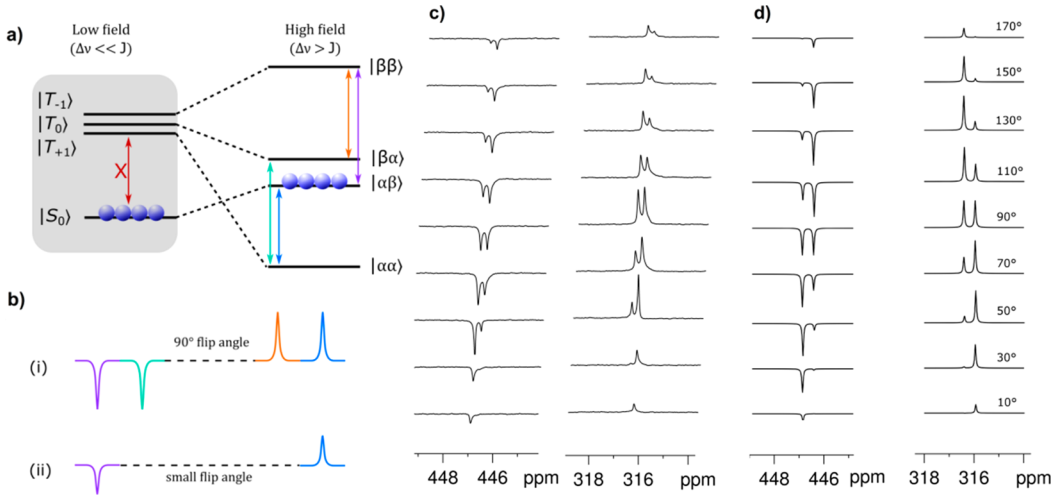

Figure 4. (a) Schematic depiction of a singlet order spin population for an inequivalent pair of coupled nuclear spins after hyperpolarization transfer in low field alongside the corresponding high-field populations after adiabatic transfer to high field. (b) Corresponding color-coded NMR spectral patterns predicted at high field after applying (i) a hard 90° flip angle pulse (purple, green, orange, and blue transitions in the above energy diagram) and (ii) a 10° flip angle pulse (purple and blue transitions). (c) $^{15}N\{^{1}H\}$ NMR spectra of a CD_3OD reaction mixture containing the catalyst **1**, diazirine **2**, and pyr-d_5. The solution was photolyzed before the acquisition of every spectrum that was hyperpolarized by 20 s of bubbling with *p*-H_2. The pulse angle is increased from 10° to 170°, bottom to top. (d) SpinDynamica[47,48] simulated $^{15}N\{^{1}H\}$ spectra for **4** assuming "pure" singlet order in the coupled $^{15}N-^{15}N$ system observed again by variable flip angle pulses of 10−170° in steps of 20° (bottom to top).

Scheme 5). These chemical shift values are consistent with those reported in the literature for this type of compound.[42,43] The generation of **2** in a nuclear singlet state is revealed through its photochemical conversion to **4** as the originally equivalent ^{15}N nuclei now become inequivalent.

Figure 4 describes the evolution of the singlet state from low to high magnetic field. The singlet order will evolve under the depicted adiabatic pathways (Figure 4a) during this transfer to overpopulate the $|\alpha\beta\rangle$ state. However, a 90° degree pulse will result in the signal shown in Figure 4b(i) where the four possible transitions are depicted in the color-coded energy level diagram. Thus, the best way to probe the singlet state is by applying a small flip angle pulse (avoiding the apparent coherence of the $|\alpha\beta\rangle$ and $|\beta\alpha\rangle$ states) and only detecting the outer transitions, which are derived from the selective population of the $|\alpha\beta\rangle$ state (Figure 4b(ii)).[44−46] The resulting spectral pattern will therefore depend on the magnitude of the pulse flip angle. Figure 4d shows the SpinDynamica[47,48] simulated NMR spectra of **4** according to the transitions of Figure 4a. Experimental findings show the predicted change in inner and outer peak intensities (Figure 4c). This behavior is striking evidence for these resonances being derived from a true singlet state.

We have already established that ^{1}H hyperpolarization transfer proceeds through nitrogen by reference to the parent diazirine. Analysis of the corresponding ^{1}H NMR spectrum after irradiation showed the appearance of hyperpolarized peaks for the CH_3 and CH_2 groups, which are adjacent to ^{15}N in the diazo-product **4**. These resonances displayed a coupling of 2.4 Hz, which disappears when ^{15}N is decoupled (see the Supporting Information). They are only visible under photolytic conditions indicating that transfer from the singlet state into these ^{1}H resonances occurs.[49−51]

The detection of alkyl diazo-compounds has been achieved previously by time-resolved techniques and by matrix photochemistry.[1,17] Very few of these compounds are isolable as a result of their extreme reactivity, and therefore they have not generally been characterized by NMR spectroscopy. Our success in using NMR spectroscopy to detect **4** is the result of combining the benefits of hyperpolarization and the long-lived singlet state character of **2**. It should be noted that when the same experiment is performed employing the diazirine with the carboxylic acid group instead of the OTBS, the diazo-species was not detected, probably due to high reactivity and very short lifetime.

Diazoalkane **4** can also be detected when this reaction is performed in an NMR tube rather than a flow reactor under hyperpolarized conditions. The sealed nature of the system results in the detection of an extra resonance at δ 309 for *ortho*-$^{15}N_2$ alongside those for **4** (see the Supporting Information); we hypothesize that N_2 gas is formed in a nonequilibrium state. The observation of N_2 is consistent with the predicted photochemistry of **2**, and concomitant formation of the corresponding carbene is required. Both CD_3OD and pyr-d_5 would be predicted to trap this intermediate under these reaction conditions.[20,21,30,52] The presence of the methanol adduct was confirmed by LIFDI mass spectrometry analysis of the reaction mixture after photolysis (see the Supporting Information). We can therefore conclude that the formation of **4** runs alongside that of the carbene and N_2, which also can be produced from **4**.

Further control experiments were performed to validate these pathways. First, no hyperpolarization was observed in the absence of the iridium catalyst or pyridine, either with or without photolysis. In addition, diazo-**4** could only be detected by NMR through its hyperpolarized response. A second set of measurements was then made on a CD_3OD solution containing the catalyst **1**, the diazirine **2**, and pyr-d_5 that was flushed with *p*-H_2 for 20 s before 20 s of photolysis without further *p*-H_2 bubbling (Figure 5a). At this point, the solution was transferred to the NMR spectrometer, and a $^{15}N\{^{1}H\}$ NMR spectrum recorded. Hyperpolarized resonances for **4** were now readily detected with both a 90° and a 30° pulse. More importantly, if the solution was sent back into the mixing chamber and rephotolyzed with no further *p*-H_2 bubbling, resonances for **4** could still be detected at high field (30°

DOI: 10.1021/jacs.8b10923
J. Am. Chem. Soc. 2018, 140, 16855−16864

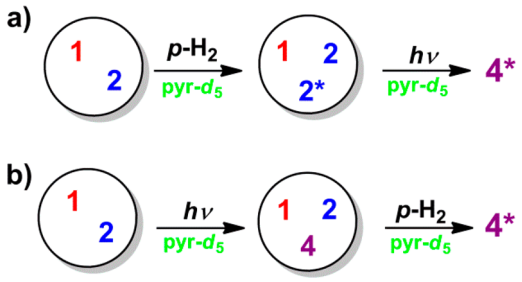

Figure 5. Schematic illustrating the steps in the control experiments elucidating the source and mechanism of hyperpolarization of **4** (the asterisks denote the hyperpolarized state of **2** and **4**).

pulse) even 90 s after initial singlet state preparation with 20% of the original signal intensity. Their appearance was again indicative of singlet state behavior (i.e., only outer peaks observed; see the Supporting Information). This confirms that the singlet state in diazirine **2** can be unlocked by photochemical conversion to **4**.

Furthermore, the same enhanced resonances of **4** were observed if the reaction mixture was photolyzed prior to bubbling with p-H_2 (Figure 5b). Additionally, compound **4** could still be detected if the resulting solution was repolarized by flushing p-H_2 through the previously irradiated solution. Hence, it can be concluded that diazo-**4** can also be polarized by SABRE through its reversible coordination to iridium in a way similar to that of **2**. This is not unexpected as diazo-compounds have been reported to act as good coordinating ligands.[53] However, the diazo-compound **4** cannot be hyperpolarized in the absence of pyridine.[15] We therefore propose a complex of the type $[Ir(H)_2(IMes)(py)_2(\mathbf{4})]Cl$ to be the SABRE active catalyst. We noted, however, that the expected PHIP-enhanced hydride signals for the $[Ir(H)_2(IMes)(py)_2(\mathbf{4})]Cl$ are not visible even at 253 K. Hence, very weak substrate binding or very fast ligand exchange is indicated.

Additional evidence for the formation of **4** was achieved by adding *N*-phenyl maleimide to the reaction mixture, which is well-known to act as a trapping agent for diazo-species.[54,55] The resulting 1,3-dipolar cycloaddition reaction affords bicyclic pyrazoline (**5a** and **5b**) in a 1:0.9 ratio of the diastereomers (Figure 6a). The ^{15}N resonances for one diastereomer were observed at δ 509.2 and δ 462.2 (d, J_{NN} = 16 Hz); the second isomer displayed peaks at δ 508.8 and δ 461.8 (d, J_{NN} = 16 Hz) in this $^{15}N\{^1H\}$ NMR spectrum. However, as these products are now stable, they can subsequently be detected by normal NMR. The same bicyclic pyrazoline product ratio was determined under these non-hyperpolarized conditions, and no peaks for **4** were visible, confirming its instability and conversion into **5** (Figure 6b). We therefore conclude that the hyperpolarization levels exhibited by these secondary reaction products are indicative of their proportions. Thus, a common reaction pathway involving both retention of nuclear spin-correlation and diamagnetic electron-spin pair transfer during the cycloaddition reaction is indicated.[56] These deductions are based on the up/down resonance phases seen for the ^{15}N NMR peaks of **5a** and **5b**, which indicate they derive from an initial singlet state.

Compounds **5a** and **5b** were again found to repolarize when p-H_2 was flushed through the solution, thereby proving their ability also to coordinate to 16-electron $[Ir(H)_2(IMes)(py)_2]Cl$. Logically, these results demonstrate that the nuclear singlet state of **2** is retained during its conversion first to **4** and then to **5**. We have therefore established the potential of such a hyperpolarization route to track a complex multistep organic reaction.[57−60]

Chemical and Nuclear Spin Order Lifetimes. The singlet state lifetime T_S of the NMR invisible state of **2** can be probed indirectly via photochemistry once it has been successfully prepared by SABRE. To do this, a sample was subject to initial p-H_2 polarization (20 s) prior to the cycling of low field photolysis and subsequent high field NMR detection of **4**. Our estimate of the resulting lifetime of **2** is 17 ± 3 s (at 9.4 T), which lies close to that previously reported for related species under these reaction conditions.[15,16] Unfortunately, we were able to collect only three points, which gives us the estimated value with large error (see the Supporting Information). Theis et al. have also demonstrated that the lifetimes of such states can be extended by storage at an appropriate low field.[15]

However, this situation is complicated by the fact that **4** should be unstable. We probed its lifetime T_S directly by NMR. This involved a series of measurements where the sample was photolyzed for 20 s with concomitant p-H_2 bubbling in the Earth's magnetic field prior to storage at the same field for a set time before subsequent transfer into the high field for observation. After FID acquisition, the solution was left for a further 60 s in the NMR spectrometer to ensure full relaxation prior to transfer back to the mixing chamber.

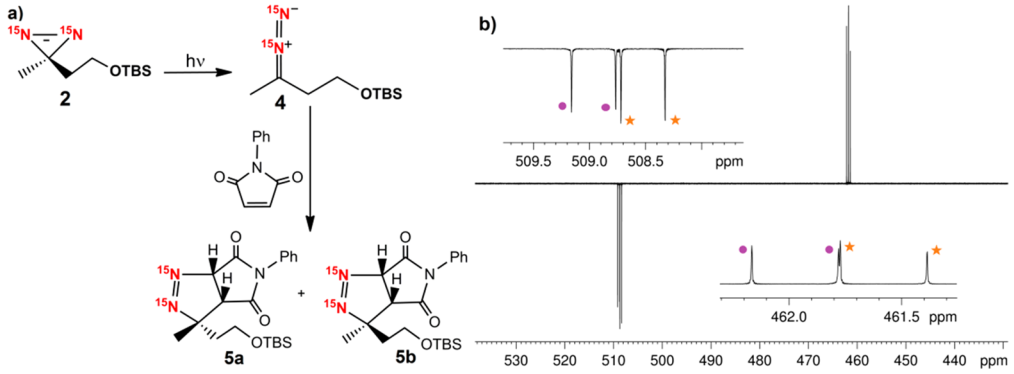

Figure 6. (a) Schematic showing the products of a 1,3 dipolar cycloaddition reaction between the diazocompound **4** and *N*-phenyl maleimide; and (b) $^{15}N\{^1H\}$ NMR spectrum of the reaction mixture with trapping agent. The dots and the stars refer to the two inequivalent ^{15}N responses of each diastereomer. The peaks are split because of the mutual ^{15}N couplings.

DOI: 10.1021/jacs.8b10923
J. Am. Chem. Soc. 2018, 140, 16855−16864

The resulting NMR spectra are shown in Figure 7 as the set time is increased from 0.25 to 45 s. The photolysis step converts a small and essentially equivalent amount of **2** into **4** each time. Thus, the only difference between these experiments is the amount of time that the solution waits in the Earth's magnetic field before transfer to high field for monitoring. To confirm reproducibility, the same set of experiments was repeated in reverse, starting with the longest set time to the shortest (see the Supporting Information). The resulting signal decays were fit to a single exponential function with an average T_S value for compound **4** at Earth's magnetic field storage of 12 ± 1 s (Figure 8a,b).

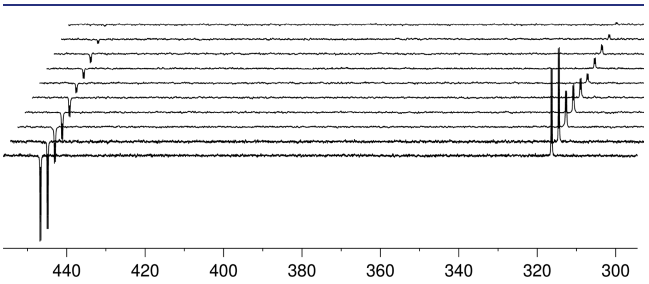

Figure 7. Series of $^{15}N\{^1H\}$ NMR spectra of a CD_3OD solution of the photochemically generated diazo-compound **4** with encoding times of 0.25, 2, 5, 8, 12, 16, 25, 30, 35, and 45 s (from bottom to top).

In a further series of measurements, the activated reaction mixture was first photolyzed for 20 s with *p*-H_2 bubbling through it. After this time, the solution was transferred to the spectrometer and a $^{15}N\{^1H\}$ measurement completed. These spectra were acquired consecutively with a small flip angle pulse (30°) and a delay of 1.05 s between them. The resulting signal intensity decay was then fit to an exponential function (see the Supporting Information) to determine the T_S of **4** at high field (9.4 T), which was 12 ± 3 s.

This process involving a single photolysis period was then repeated with repolarization. To do this, a sample was photolyzed for 20 s under *p*-H_2 prior to making an initial $^{15}N\{^1H\}$ measurement. The solution was then transferred back to the mixing chamber and *p*-H_2 added for 20 s before being sent back to the NMR spectrometer for FID acquisition. This sequence was repeated until no signal for **4** could be observed. In this way, we used the hyperpolarization of **4** to determine its chemical lifetime. These data were fitted to an exponential decay, and a chemical lifetime of 100 ± 5 s was estimated (Figure 8c,d). Our attempts to determine the chemical lifetime of **4** by UV−vis spectroscopy were unsuccessful, although we observed bleaching due to the consumption of **2**.

Implications for the Formation of *para*-N_2. We exploited the NMR signal integration of **5a** and **5b** formed in the cycloaddition process (Figure 6) to assess the ratio of N_2 production versus the formation of the diazo-**4**. At 33% consumption of **2**, where the products **5a** and **5b** account for 19%, the peak for *ortho* $^{15}N_2$ is 4% of the original signal for **2** (as derived from integration of the ^{15}N spectrum under Boltzman conditions). The 10% of unassigned product could be rationalized by further N_2 gas in the head space of the NMR

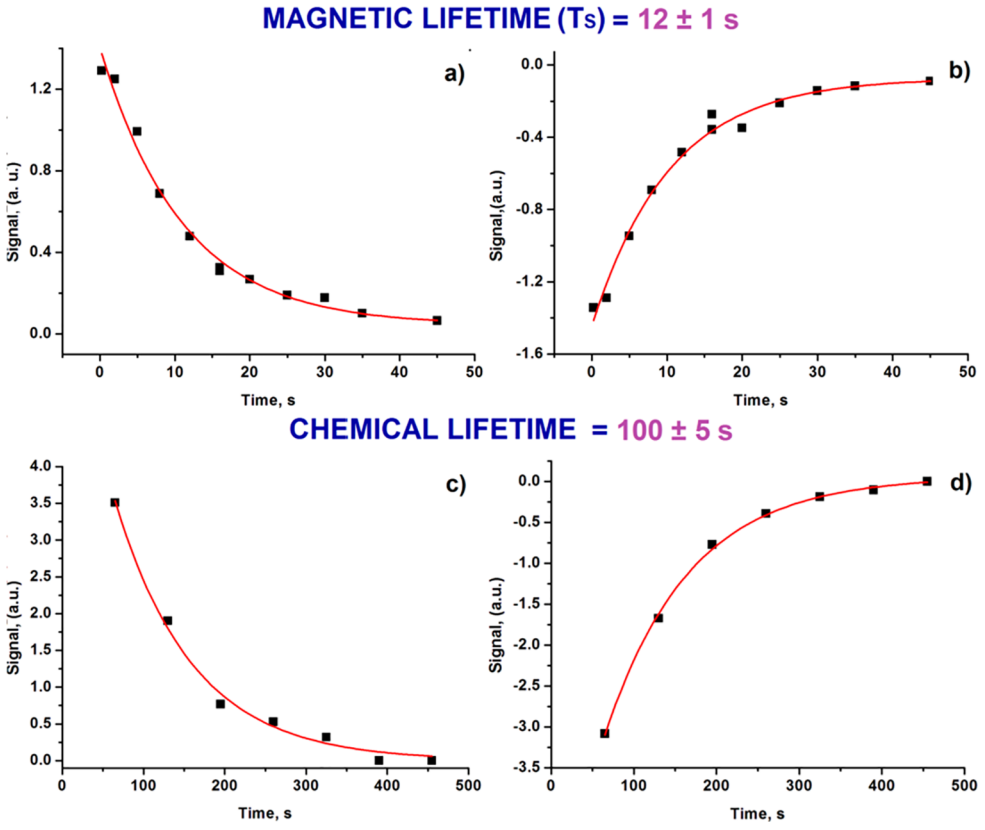

Figure 8. (a,b) Decay of signal intensity measurements for **4** after hyperpolarization and storage at low field in CD_3OD solution prior to read-out. Points acquired from the shortest time to the longest. (c,d) Decay of signal intensity measurements for **4** in CD_3OD solution with repolarization of the reaction mixture, which was photolyzed once prior to the first point. In all cases, ■ are the experimental points obtained by integrating the $^{15}N\{^1H\}$ NMR signal of compound **4**, while red lines of best fit are added via an exponential decay function.

DOI: 10.1021/jacs.8b10923
J. Am. Chem. Soc. 2018, 140, 16855−16864

tube (or by the NMR silent p-N_2, see the Supporting Information). These results indicate an approximate 1:1 ratio for N_2 liberation and photoisomerization processes assuming similar relaxation rates of ^{15}N for the different species (see the Supporting Information). The observation of polarized N_2 at δ 309 corroborates the potential formation of p-N_2, the singlet nuclear spin isomer of N_2 if the singlet state of **2** is preserved throughout the photochemical process. The detection of the hyperpolarized cycloaddition products (Figure 9, paths A and D) confirms retention of hyperpolarization. Similar reasoning has been used to justify p-N_2 generation by others.[37] Unfortunately, while diazo-**4** was predicted to form by both photoisomerization (Figure 9, path A) and the recombination of N_2 and the carbene[17] (Figure 9, pathways B and C), we see no difference in product distribution when the photolysis step is performed under an N_2 atmosphere. Therefore, we cannot attribute the detection of hyperpolarized **4** to the intermolecular recombination pathway (Figure 9, pathways B and C). We note that p-N_2 can be formed by the direct route B of Figure 9 or as a secondary photoproduct via routes A and C. In either of these mechanisms, the p-N_2 signal will however be NMR silent as it is perfectly symmetric and nonmagnetic in nature.

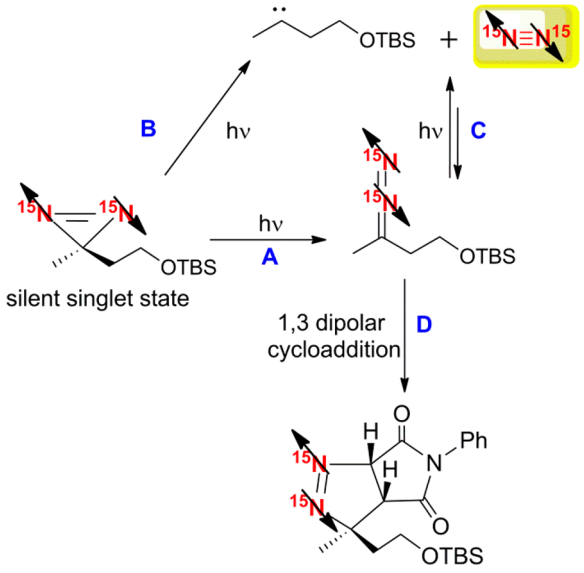

Figure 9. Reaction scheme summarizing the different pathways to the generation of p-N_2.

CONCLUSIONS

In this Article, we have successfully used photochemistry to unlock the detection of a silent magnetic singlet state in $^{15}N_2$-OTBS-diazirine **2** that was created via the SABRE mechanism (estimated T_S at 9.4 T of 17 ± 3 s). Catalyst **3** of Scheme 4 with bound hydride, pyridine, and diazirine ligands was characterized by NMR spectroscopy and identified to play a key role in this step. The photoisomerization of **2** afforded unstable diazo-**4** of Scheme 5, which was also characterized in solution by NMR spectroscopy. The T_S of **4** was determined both at low field (≃500 mG) and at high field (9.4 T) to be 12 ± 1 s. This lifetime is relatively insensitive to the strength of the magnetic field. The nature of the singlet state of **4** has been validated by controlled radio frequency excitation and filtration experiments with the theoretical simulations detailed matching perfectly with the experimental findings. In contrast, the chemical lifetime of **4** is 100 ± 5 s and therefore substantially longer than its magnetic state lifetime.

We have further shown that **4** can be trapped by a suitable agent to afford complexes **5a** and **5b**. Remarkably, this process retains both hyperpolarization and singlet state in the products, indicating a 1,3-dipolar cycloaddition which must involve spin correlated electron transfer. Hence, we have established that hyperpolarization is a potential route to rationalize the outcome of organic pericyclic reactions. The different pathways for the photodecomposition of **2** are analyzed to account for generation of N_2 and support the formation of p-N_2. We are seeking to obtain more direct evidence for the formation of p-N_2 and plan to exploit its hyperpolarization potential.

ASSOCIATED CONTENT

Supporting Information

The Supporting Information is available free of charge on the ACS Publications website at DOI: 10.1021/jacs.8b10923. Raw NMR data can be downloaded at DOI 10.15124/8de06fe8-ea9d-49ff-bdd4-bb13cf605de5.

NMR characterization data, additional spectra, theoretical analysis, synthetic methods, and further technical descriptions (DOCX)

AUTHOR INFORMATION

Corresponding Author

*simon.duckett@york.ac.uk

ORCID

Barbara Procacci: 0000-0001-7044-0560
Soumya S. Roy: 0000-0002-9193-9712
Philip Norcott: 0000-0003-4082-2079
Norman Turner: 0000-0001-5089-6704
Simon B. Duckett: 0000-0002-9788-6615

Notes

The authors declare no competing financial interest.

ACKNOWLEDGMENTS

An anonymous donor, the Wellcome Trust (092506 and 098335), the University of York, and the EPSRC (EP/R51181X/1) are thanked for supporting this work. We thank Dr. Peter Rayner and Dr. Richard John for experimental help. Professor Robin N. Perutz, Dr. Pedro Aguiar, and Dr. William Unsworth are also acknowledged for stimulating discussions.

REFERENCES

(1) Korneev, S. M. Valence isomerization between diazo compounds and diazirines. *Eur. J. Org. Chem.* **2011**, *2011*, 6153.
(2) Griffin, G. W. Generation of carbenes by photochemical cycloelimination. *Angew. Chem., Int. Ed. Engl.* **1971**, *10*, 537.
(3) Frey, H. M.; Stevens, I. D. R. Photolysis of dimethyldiazirine. *J. Chem. Soc.* **1963**, 3514.
(4) Morandi, B.; Carreira, E. M. Iron-catalyzed cyclopropanation in 6 M KOH with in situ generation of diazomethane. *Science* **2012**, *335*, 1471.
(5) Mix, K. A.; Aronoff, M. R.; Raines, R. T. Diazo compounds: versatile tools for chemical biology. *ACS Chem. Biol.* **2016**, *11*, 3233.
(6) Andersen, K. A.; Aronoff, M. R.; McGrath, N. A.; Raines, R. T. Diazo groups endure metabolism and enable chemoselectivity in cellulo. *J. Am. Chem. Soc.* **2015**, *137*, 2412.

DOI: 10.1021/jacs.8b10923
J. Am. Chem. Soc. 2018, 140, 16855−16864

(7) McGrath, N. A.; Andersen, K. A.; Davis, A. K. F.; Lomax, J. E.; Raines, R. T. Diazo compounds for the bioreversible esterification of proteins. *Chem. Sci.* **2015**, *6*, 752.
(8) Sumranjit, J.; Chung, S. J. Recent advances in target characterization and identification by photoaffinity probes. *Molecules* **2013**, *18*, 10425.
(9) Dubinsky, L.; Krom, B. P.; Meijler, M. M. Diazirine based photoaffinity labeling. *Bioorg. Med. Chem.* **2012**, *20*, 554.
(10) Hall, M. A.; Xi, J.; Lor, C.; Dai, S. P.; Pearce, R.; Dailey, W. P.; Eckenhoff, R. G. m-Azipropofol (AziPm) a photoactive analogue of the intravenous general anesthetic propofol. *J. Med. Chem.* **2010**, *53*, 5667.
(11) Liebmann, M.; Di Pasquale, F.; Marx, A. A new photoactive building block for investigation of DNA backbone interactions: photoaffinity labeling of human DNA polymerase beta. *ChemBioChem* **2006**, *7*, 7−1965.
(12) Suchanek, M.; Radzikowska, A.; Thiele, C. Photo-leucine and photo-methionine allow identification of protein-protein interactions in living cells. *Nat. Methods* **2005**, *2*, 261.
(13) Kinoshita, T.; Cano-Delgado, A. C.; Seto, H.; Hiranuma, S.; Fujioka, S.; Yoshida, S.; Chory, J. Binding of brassinosteroids to the extracellular domain of plant receptor kinase BRI1. *Nature* **2005**, *433*, 167.
(14) Chan, E. W. S.; Chattopadhaya, S.; Panicker, R. C.; Huang, X.; Yao, S. Q. Developing photoactive affinity probes for proteomic profiling: hydroxamate-based probes for metalloproteases. *J. Am. Chem. Soc.* **2004**, *126*, 14435.
(15) Theis, T.; Ortiz, G. X.; Logan, A. W. J.; Claytor, K. E.; Feng, Y.; Huhn, W. P.; Blum, V.; Malcolmson, S. J.; Chekmenev, E. Y.; Wang, Q.; Warren, W. S. Direct and cost-efficient hyperpolarization of long-lived nuclear spin states on universal $^{15}N_2$-diazirine molecular tags. *Sci. Adv.* **2016**, *2*, e1501438.
(16) Shen, K.; Logan, A. W. J.; Colell, J. F. P.; Bae, J.; Ortiz, G. X.; Theis, T.; Warren, W. S.; Malcolmson, S. J.; Wang, Q. Diazirines as potential molecular imaging tags: probing the requirements for efficient and long-lived SABRE-induced hyperpolarization. *Angew. Chem., Int. Ed.* **2017**, *56*, 12112.
(17) Moore, C. B.; Pimentel, G. C. Matrix reaction of methylene with nitrogen to form diazomethane. *J. Chem. Phys.* **1964**, *41*, 3504.
(18) Ammann, J. R.; Subramanian, R.; Sheridan, R. S. Dicyclopropylcarbene - direct characterization of a singlet dialkylcarbene. *J. Am. Chem. Soc.* **1992**, *114*, 7592.
(19) Seburg, R. A.; Mcmahon, R. J. Photochemistry of matrix-isolated diazoethane and methyldiazirine - ethylidene trapping. *J. Am. Chem. Soc.* **1992**, *114*, 7183.
(20) Modarelli, D. A.; Morgan, S.; Platz, M. S. Carbene formation, hydrogen migration, and fluorescence in the excited-states of dialkyldiazirines. *J. Am. Chem. Soc.* **1992**, *114*, 7034.
(21) Modarelli, D. A.; Platz, M. S. Interception of dimethylcarbene with pyridine - a laser flash-photolysis study. *J. Am. Chem. Soc.* **1991**, *113*, 8985.
(22) Amrich, M. J.; Bell, J. A. Photoisomerization of diazirine. *J. Am. Chem. Soc.* **1964**, *86*, 292.
(23) Yamamoto, N.; Bernardi, F.; Bottoni, A.; Olivucci, M.; Robb, M. A.; Wilsey, S. Mechanism of carbene formation from the excited-states of diazirine and diazomethane - an MC-SCF Study. *J. Am. Chem. Soc.* **1994**, *116*, 2064.
(24) Haselbach, E.; Heilbron, E.; Mannschr, A.; Seitz, W. Applications of photoelectron spectroscopy. Lone pair interaction in 3,3-dimethyldiazirine. *Angew. Chem., Int. Ed. Engl.* **1970**, *9*, 902.
(25) Kochanski, E.; Lehn, J. M. Electronic structure of cyclopropane, cyclopropene and diazirine an Ab Initio SCF-LCAO-MO study. *Theor. Chim. Acta* **1969**, *14*, 281.
(26) Shur, V. B.; Tikhonova, I. A.; Aleksandrov, G. G.; Struchkov, Y. T.; Volpin, M. E.; Schmitz, E.; Jahnisch, K. The diazirine complex $[(NH_3)_5Ru(N_2C_6H_{10})]^{2+}$ - Synthesis, structure and conversion into the dinitrogen complex $[(NH_3)_5RuN_2]^{2+}$. *Inorg. Chim. Acta* **1980**, *44*, L275.
(27) Albini, A.; Kisch, H. Transition-metal complexes of azo-compounds. Complexation and cleavage of N = N bond of diazirines by iron carbonyls. *J. Organomet. Chem.* **1975**, *94*, 75.
(28) Roy, J. R.; Monim, S. S.; Mcbreen, P. H. Totally selective NN bond-cleavage in the dissociative adsorption of diazirine on Cu(110). *J. Am. Chem. Soc.* **1994**, *116*, 11883.
(29) Mcbreen, P. H.; Roy, J. R.; Monim, S. S. Non-synergistic pi-sigma chemisorption bonding - CH_2N_2 on Pd(110) and Cu(110). *Chem. Phys. Lett.* **1994**, *223*, 481.
(30) Barra, M.; Fisher, T. A.; Cernigliaro, G. J.; Sinta, R.; Scaiano, J. C. On the photodecomposition mechanism of ortho-diazonaphthoquinones. *J. Am. Chem. Soc.* **1992**, *114*, 2630.
(31) Avent, A. G.; Benyunes, S. A.; Chaloner, P. A.; Hitchcock, P. B. Synthesis of mu-carbene complexes of rhodium from substituted diazirines. *J. Chem. Soc., Chem. Commun.* **1987**, 1285.
(32) Benyunes, S. A.; Chaloner, P. A. Synthesis of mu-carbene complexes of cobalt from substituted diazirines. *J. Organomet. Chem.* **1988**, *341*, C50.
(33) Avent, A. G.; Benyunes, S. A.; Chaloner, P. A.; Gotts, N. G.; Hitchcock, P. B. Synthesis of mu-carbene and mu-carbyne complexes of rhodium and cobalt from substituted diazirines - crystal-structures of $[Rh_2(eta^5\text{-}C_5Me_5)_2(CO)_2[\mu\text{-}C(C_6H_4F_4)(OMe)]]$ and $[Rh_2(\eta^5\text{-}C_5Me_5)_2(\mu\text{-}CO)(\mu\text{-}C_6H_4Me_4)][BPh_4]$. *J. Chem. Soc., Dalton Trans.* **1991**, 1417.
(34) Bowers, C. R.; Weitekamp, D. P. Para-hydrogen and synthesis allow dramatically enhanced nuclear alignment. *J. Am. Chem. Soc.* **1987**, *109*, 5541.
(35) Eisenschmid, T. C.; Kirss, R. U.; Deutsch, P. P.; Hommeltoft, S. I.; Eisenberg, R.; Bargon, J.; Lawler, R. G.; Balch, A. L. Para hydrogen induced polarization in hydrogenation reactions. *J. Am. Chem. Soc.* **1987**, *109*, 8089.
(36) Adams, R. W.; Aguilar, J. A.; Atkinson, K. D.; Cowley, M. J.; Elliott, P. I. P.; Duckett, S. B.; Green, G. G. R.; Khazal, I. G.; Lopez-Serrano, J.; Williamson, D. C. Reversible interactions with para-hydrogen enhance NMR sensitivity by polarization transfer. *Science* **2009**, *323*, 1708.
(37) Bae, J. N.; Zhou, Z. J.; Theis, T.; Warren, W. S.; Wang, Q. $^{15}N_4$-1,2,4,5-tetrazines as potential molecular tags: integrating bioorthogonal chemistry with hyperpolarization and unearthing para-N_2. *Sci. Adv.* **2018**, *4*, eaar2978.
(38) Cowley, M. J.; Adams, R. W.; Atkinson, K. D.; Cockett, M. C. R.; Duckett, S. B.; Green, G. G. R.; Lohman, J. A. B.; Kerssebaum, R.; Kilgour, D.; Mewis, R. E. Iridium N-heterocyclic carbene complexes as efficient catalysts for magnetization transfer from para-hydrogen. *J. Am. Chem. Soc.* **2011**, *133*, 6134.
(39) Lloyd, L. S.; Adams, R. W.; Bernstein, M.; Coombes, S.; Duckett, S. B.; Green, G. G. R.; Lewis, R. J.; Mewis, R. E.; Sleigh, C. J. Utilization of SABRE-derived hyperpolarization to detect low-concentration analytes via 1D and 2D NMR methods. *J. Am. Chem. Soc.* **2012**, *134*, 12904.
(40) Mewis, R. E.; Atkinson, K. D.; Cowley, M. J.; Duckett, S. B.; Green, G. G. R.; Green, R. A.; Highton, L. A. R.; Kilgour, D.; Lloyd, L. S.; Lohman, J. A. B.; Williamson, D. C. Probing signal amplification by reversible exchange using an NMR flow system. *Magn. Reson. Chem.* **2014**, *52*, 358.
(41) Wagner, S. Conversion rate of para-hydrogen to ortho-hydrogen by oxygen: implications for PHIP gas storage and utilization. *MAGMA* **2014**, *27*, 195.
(42) Lown, J. W.; Chauhan, S. M. S.; Koganty, R. R.; Sapse, A. M. Alkyldinitrogen species implicated in the carcinogenic, mutagenic, and anticancer activities of N-nitroso compounds - characterization by ^{15}N-NMR of ^{15}N-enriched compounds and analysis of DNA-base situselectivity by abinitio calculations. *J. Am. Chem. Soc.* **1984**, *106*, 6401.
(43) Duthaler, R. O.; Forster, H. G.; Roberts, J. D. ^{15}N and ^{13}C Nuclear magnetic-resonance spectra of diazo and diazonium compounds. *J. Am. Chem. Soc.* **1978**, *100*, 4974.
(44) Tayler, M. C. D.; Marco-Rius, I.; Kettunen, M. I.; Brindle, K. M.; Levitt, M. H.; Pileio, G. Direct enhancement of nuclear singlet

DOI: 10.1021/jacs.8b10923
J. Am. Chem. Soc. 2018, 140, 16855−16864

order by dynamic nuclear polarization. *J. Am. Chem. Soc.* **2012**, *134*, 7668.
(45) Natterer, J.; Bargon, J. Parahydrogen induced polarization. *Prog. Nucl. Magn. Reson. Spectrosc.* **1997**, *31*, 293.
(46) Pravica, M. G.; Weitekamp, D. P. Net NMR alignment by adiabatic transport of para-hydrogen addition-products to high magnetic-field. *Chem. Phys. Lett.* **1988**, *145*, 255.
(47) Bengs, C.; Levitt, M. H. Spindynamica: symbolic and numerical magnetic resonance in a mathematica environment. *Magn. Reson. Chem.* **2018**, *56*, 374.
(48) Wolfram Research, I. *Mathematica, Version 11.0*; Wolfram Research, Inc.: Champaign, IL, 2018.
(49) Roy, S. S.; Appleby, K. M.; Fear, E. J.; Duckett, S. B. SABRE-Relay: a versatile route to hyperpolarization. *J. Phys. Chem. Lett.* **2018**, *9*, 1112.
(50) Roy, S. S.; Norcott, P.; Rayner, P. J.; Green, G. G. R.; Duckett, S. B. A Hyperpolarizable ^{1}H magnetic resonance probe for signal detection 15 minutes after spin polarization storage. *Angew. Chem., Int. Ed.* **2016**, *55*, 15642.
(51) Roy, S. S.; Rayner, P. J.; Norcott, P.; Green, G. G. R.; Duckett, S. B. Long-lived states to sustain SABRE hyperpolarised magnetisation. *Phys. Chem. Chem. Phys.* **2016**, *18*, 24905.
(52) Creary, X.; Butchko, M. A. beta-silylcarbenes from isolable diazosilanes. *J. Org. Chem.* **2002**, *67*, 112.
(53) Alvarez, M. A.; Garcia, M. E.; Garcia-Vivo, D.; Huergo, E.; Ruiz, M. A.; Vega, M. F. Thermally Stable diazoalkane derivatives of the unsaturated ditungsten hydride $[W_2Cp_2(H)(eta\text{-}PCy_2)(CO)_2]$. *Organometallics* **2015**, *34*, 3833.
(54) Stevens, I. D. R.; Liu, M. T. H.; Soundararajan, N.; Paike, N. The thermal-decomposition of diazirines - 3-(3-methyldiazirin-3-yl)propan-1-ol and 3-(3-Methyldiazirin-3-Yl)propanoic acid. *J. Chem. Soc., Perkin Trans. 2* **1990**, *2*, 661.
(55) Molchanov, A. P.; Diev, V. V.; Kostikov, R. R. Reactions of aliphatic diazo compounds: IV. Reaction of diphenyldiazomethane with substituted Imides of maleic and itaconic acids. *Russ. J. Org. Chem.* **2002**, *38*, 259.
(56) Huisgen, R. Kinetik Und Mechanismus 1.3-Dipolarer Cycloadditionen. *Angew. Chem.* **1963**, *75*, 742.
(57) Battilocchio, C.; Feist, F.; Hafner, A.; Simon, M.; Tran, D. N.; Allwood, D. M.; Blakemore, D. C.; Ley, S. V. Iterative reactions of transient boronic acids enable sequential C-C bond formation. *Nat. Chem.* **2016**, *8*, 360.
(58) Poh, J. S.; Tran, D. N.; Battilocchio, C.; Hawkins, J. M.; Ley, S. V. A Versatile room-temperature route to di- and trisubstituted allenes using flow-generated diazo compounds. *Angew. Chem., Int. Ed.* **2015**, *54*, 7920.
(59) Tran, D. N.; Battilocchio, C.; Lou, S. B.; Hawkins, J. M.; Ley, S. V. Flow chemistry as a discovery tool to access sp^2-sp^3 cross-coupling reactions via diazo compounds. *Chem. Sci.* **2015**, *6*, 1120.
(60) Aronoff, M. R.; Gold, B.; Raines, R. T. 1,3-Dipolar cycloadditions of diazo compounds in the presence of azides. *Org. Lett.* **2016**, *18*, 1538.

DOI: 10.1021/jacs.8b10923
J. Am. Chem. Soc. 2018, 140, 16855−16864